

Synthesis and Characterization of Maleated Glycidyl 3-Pentadecenyl Phenyl Ether as a Functionalized Plasticizer for Styrene-Butadiene Rubber/Carbon Black/Silica Composites

Zhan-Lin Gong, Lan Cen, Shu-Ting Wang, Fu-Lin Chen

School of Materials and Energy, Guangdong University of Technology, Guangzhou 510006, China

Correspondence to: Z.-L. Gong (E-mail: samuel823@foxmail.com)

ABSTRACT: Maleated glycidyl 3-pentadecenyl phenyl ether (M-GPPE) was synthesized from glycidyl 3-pentadecenyl phenyl ether (GPPE), a renewable derivative from cardanol, with maleic anhydride (MAH) by grafting copolymerization. The resulting M-GPPE was used as a functionalized plasticizer for a styrene-butadiene rubber (SBR)/carbon black (CB)/silica composite. The effects of M-GPPE on the development of the filler network, the extent of silica dispersion, the curing characteristics, and the mechanical performance of the composites were studied. Meanwhile, a comparative study was performed between M-GPPE and aromatic oil, a traditional plasticizer used in SBR filler formulations. Gel permeation chromatography and IR and ¹H-NMR analysis results confirmed the occurrence of the grafting reaction between GPPE and MAH and the potential structure of M-GPPE. The thermostability of GPPE was improved by grafting copolymerization with MAH, as shown by thermogravimetric analysis results. The presence of M-GPPE resulted in a shorter curing time and better aging properties in the SBR composite compared with GPPE. The mechanical properties, dynamic mechanical analysis, and transmission electron microscopy analysis showed that the maleate of GPPE could enhance the compatibility between SBR and silica, improve the dispersion of silica in SBR, and partially replace the aromatic oil in the SBR/CB/silica composite formulation. © 2014 Wiley Periodicals, Inc. *J. Appl. Polym. Sci.* **2014**, *131*, 40462.

KEYWORDS: applications; compatibilization; copolymers; radical polymerization; rubber

Received 19 July 2013; accepted 17 January 2014

DOI: 10.1002/app.40462

INTRODUCTION

Styrene-butadiene rubber (SBR)/carbon black (CB)/silica composites are widely applied in rubber products. However, when an increased filler content is accompanied by increased filler activity, the incorporation of a higher concentration of fillers in SBR rubber results in the occurrence of filler agglomeration and the poor dispersion of filler, which is responsible for the poor processability and inferior mechanical performances of the composites. In general, to obtain a finer dispersion of filler and better mechanical performances of the composites, the presence of plasticizers and silica coupling agents in high-filler-loading compounds is necessary. It has been reported that carboxylated acrylonitrile-butadiene with a low molecular weight was used as a functional plasticizer for SBR/CB/organoclay composites,¹ a SBR/recycled acrylonitrile-butadiene rubber/CB/silica composite plasticized and reinforced by bis(γ -triethoxysilylpropyl) tetrasulfide showed a 12% tensile strength increase,² and SBR/silica composites modified by (3-glycidyoxypropyl) trimethoxysilane or *N*-phenyl-1,4-phenylenediamine showed a almost 36% tensile strength increase.³

Cashew nut shell liquid (CNSL) is a kind of renewable resource and byproduct of the cashew industry. It is suitable for various applications. The main ingredient of CNSL is cardanol, a phenol derivative containing a C₁₅ unsaturated hydrocarbon chain, which is often used as a good polymer synthetic monomer for the formation of unsaturated hydrocarbon phenol⁴⁻⁶ and a plasticizer in the plastic and rubber industry.⁷⁻⁹ In recent years, much attention has been paid to the further function of cardanol as a multifunctional additive, for example, as phosphorylated cardanol as a crosslinkable plasticizer for rubber,¹⁰ as synthesized cardanol-formaldehyde resins for the reinforcement of NR,¹¹ and in the esterification of the cardanol hydroxyl group (cardanol acetate) or further epoxidation of side-chain double bonds (epoxidized cardanol acetate) for good miscibility with poly(vinyl chloride).¹² In particular, the epoxidation of cardanol with epichlorohydrin to form glycidyl 3-pentadecenyl phenyl ether (GPPE) has been successfully used to improve the surface-coating properties of varnishes¹³ and as a functional monomer for ecofriendly vinyl ester resin systems, which combine the best properties of epoxies and unsaturated

polyesters.^{14,15} However, few researchers have used GPPE as a plasticizer or as a coupling agent in rubber/polar filler composites. With the presence of an epoxy group in the end of the GPPE chain, the application of GPPE in SBR/CB/silica composites as a functional plasticizer may improve the interaction between SBR and silica.

However, the addition of GPPE directly to the SBR matrix may cause inadequate sulfidity and a lower crosslinking density of the composite, because there is a possibility of chemical reactions between epoxy group and rubber chemicals like zinc oxide, stearic acid, accelerator and sulphur.^{16,17} Hence, in this study, maleic anhydride (MAH), which has been used as a dienophile in the preparation of adducts with a variety of diene compounds,^{18,19} was introduced to react with GPPE by grafting copolymerization to reduce the effect of epoxy groups on the compound vulcanized processing and enhance the interaction between SBR and silica. Also, GPPE, maleated glycidyl 3-pentadecenyl phenyl ether (M-GPPE), and aromatic oil were compared in SBR/CB/silica composite formulations.

EXPERIMENTAL

Materials

GPPE was donated by Cardolite Chemical Zhuhai Co., Ltd. (Zhuhai, China, concentration >99%, viscosity at 25°C = 50 cPs). MAH and benzoyl peroxide were purchased from Aladdin Industrial Corp. (Shanghai, China, concentration >99.5%). SBR 1502 was supplied by Jilin Rubber Co., Ltd. (Jilin, China, styrene content = 23.5 wt %). Aromatic oil was obtained from Sindy Chemicals Corp. (Shanghai, China, specific gravity = 0.98; viscosity gravity constant = 0.96). Other rubber additives were industrial grade and were used as received.

M-GPPE Synthesis

The dry MAH (22.5 wt %) was dissolved in GPPE (77.5 wt %) at 60°C. After complete dissolution, the initiator (benzoyl peroxide = 0.2% on basis of the weight of MAH and GPPE) was incorporated into the GPPE and MAH mixture. The reaction of GPPE grafting copolymerization with MAH was performed in a three-necked flask at 80°C at a rotor speed of 40 rpm for 2 h in a nitrogen atmosphere. After the reaction finished, the resulting mixture (M-GPPE) was cooled to room temperature and used directly.

The purification of M-GPPE was carried out for IR analysis. The M-GPPE sample was purified thoroughly with hexane in the separator funnel; then, it was dried in a vacuum oven at 60°C for 8 h to make sure that no free or physically bound MAH unit or MAH copolymer was present by means of acid–base titration.

Preparation of the SBR/CB/Silica Composites

We mixed the compounding formulations for the SBR/CB/silica composite with its various ingredients in a two-roll mill at a friction ratio of 1:2 following standard mixing sequence at room temperature. The composition [in parts per hundred parts of rubber (phr)] was as follows: SBR = 100 phr, zinc oxide (ZnO) = 5.0 phr, stearic acid = 1.5 phr, *N*-isopropyl-*N*O-phenyl-1,4-phenylenediamine (4010NA) = 1.5 phr, *N*-cyclohexyl-2-benzothiazole sulfenamide = 1.5 phr, diphenyl guanidine (DPG) = 0.6 phr, CB

(N330) = 50 phr, silica = 20 phr, sulfur = 2.5 phr, and variable plasticizer. The plasticizer was incorporated in the last compounding process. Various plasticizers, that is, aromatic oil, GPPE, and M-GPPE with different contents (5.0, 10.0, and 15.0 phr), were compared in the formulation. The curing characteristics of the compound rubber were studied with the help of a UR-2030 vulcanometer (U-CAN, Nantou, Taiwan) at 170°C. From the vulcanization curve, the optimum curing time (t_{90}) was determined. At last, the compounds were vulcanized at 170°C for t_{90} in a standard mold to produce the SBR/CB/silica composites.

Characterization

The molecular weight and polydispersity (number-average molecular weight/weight-average molecular weight) were determined by gel permeation chromatography on a 510 HPLC equipped with three polystyrene gel columns (ultrastayragel liners 103, 500, and 100 Å) with tetrahydrofuran as an eluent, a flow rate of 1.0 mL/min, polystyrene calibration, and refractive index detectors.

IR spectroscopy of GPPE and M-GPPE was studied with a PerkinElmer 843 spectrophotometer in the range 600–4000 cm^{-1} . GPPE and M-GPPE were dissolved in chloroform, and then, a film was cast on the KBr disk. The solvent was evaporated with the help of an IR lamp.

¹H-NMR spectra were recorded on a Bruker 300-MHz spectrometer with the samples, which were swollen with deuterated chloroform.

Thermogravimetric analysis (TGA) was carried out with a Q50 thermal analyzer from TA Instruments to study the effect of different contents of MAH on the thermostability of M-GPPE in comparison with raw GPPE. All of the TGA experiments were performed by the heating of the sample at a rate of 10°C/min under a nitrogen atmosphere from room temperature to 600°C.

The mechanical characterization tests of the SBR composites were done by means of a universal tensile testing machine (SANS, CMT4104, Shenzhen, China) under ambient conditions ($25 \pm 2^\circ\text{C}$). The initial length of the specimens was 25 mm, and the speed of the jaw separation was 500 mm/min. The composite aging was carried out at 120°C for 72 h.

The dynamic mechanical analysis was conducted with rectangular samples with dimensions of $12 \times 6 \times 2 \text{ mm}^3$ on a dynamic shear rheometer machine (Rheometrics model DSR5). The tests were performed at a frequency of 1 Hz with temperature programs from -40 to 80°C at a heating rate of $5^\circ\text{C}/\text{min}$. Testing was conducted in single torsion mode with mechanical stress.

Transmission electron microscopy (TEM) observations were done on ultramicrotomed slices ($\sim 200 \text{ nm}$) with a Philips Tecnai 12 transmission electron microscope (Eindhoven, The Netherlands) with an accelerating voltage of 30 kV.

RESULTS AND DISCUSSION

Polymer Properties

The M-GPPE synthesized from GPPE and MAH showed a reddish viscous liquid. The gel permeation chromatography result of the M-GPPE presented a lower molecular weight (number-

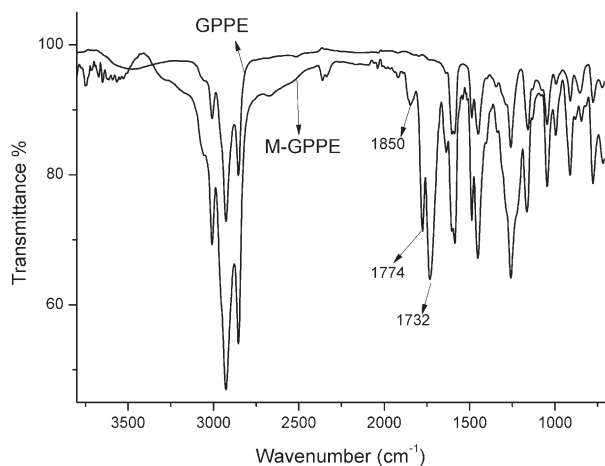


Figure 1. IR spectra of GPPE and M-GPPE.

average molecular weight = 9335, weight-average molecular weight of 12,975, and a polydispersity of 1.39).

The IR spectra of GPPE and the M-GPPE are shown in Figure 1. Both GPPE and M-GPPE exhibited the same characteristic peaks at 911, 1046, 1259, 1603, 2854, 2926, and 3008 cm^{-1} as found in other studies.^{13–15} In addition to this, in the spectrum of M-GPPE, some new additional peaks at 1732, 1774, and 1850 cm^{-1} , which were attributed to the C=O stretching vibrations of MAH,^{18,19} were present; this confirmed the grafting copolymerization reaction between GPPE and MAH. The absence of a peak at 3200–3500 cm^{-1} in M-GPPE spectrum suggested that the —OH group did not form on the M-GPPE molecular chain during the grafting copolymerization reaction.²⁰ Barton et al.²¹ reported that the non-catalyzed anhydride-epoxy curing

reaction is less reactive and hence demands a high reaction temperature to initiate the curing reaction. In addition, the presence of a conjugated diene component on GPPE might provide a reaction site to form functional products via a Diels–Alder reaction,²² but the lack of a characteristic peak of the cyclohexene group at 720 cm^{-1} in the M-GPPE spectrum excluded the occurrence of this kind of reaction between GPPE and MAH.

Therefore, a possible reaction mechanism reaction for M-GPPE is proposed in Figure 2. Three type products were extremely likely to be produced during the grafting copolymerization reaction. In the first case, as shown in Figure 2(a), the free radicals generated at the C=C bonds between the GPPE side chain and MAH would end in the termination of the double-base coupling. In the second case, allylic carbon atoms from the reaction of the initiator was one of the reactive sites for the grafting copolymerization reaction [Figure 2(b)]. These reaction mechanisms were similar to NR grafting with cardanol²⁰ and the grafting reaction between MAH and NR.²³ In the third case, the end of the GPPE side chain macroradical would attack the double bonds of MAH via addition reaction to form a copolymer [Figure 2(c)].

The ¹H-NMR spectrum of M-GPPE shown in Figure 3 presented aromatic proton peaks in the $\delta = 6.5\text{--}7.2$ ppm range. The peaks in the range $\delta = 4.9\text{--}5.4$ ppm pointed to vinyl unsaturation. The peaks in the range $\delta = 0.5\text{--}2.8$ ppm suggested the presence of alkyl chain unsaturation. The peaks at $\delta = 4.2$, 3.4, and 2.9 ppm were assigned to the glycidyl of M-GPPE. These observations were similar to the reports of Bhunia et al.²⁴ and Suresh.²⁵ The peaks between δ values 4.1 and 3.7 were due to methylene protons, which came from the saturated cyclic five-

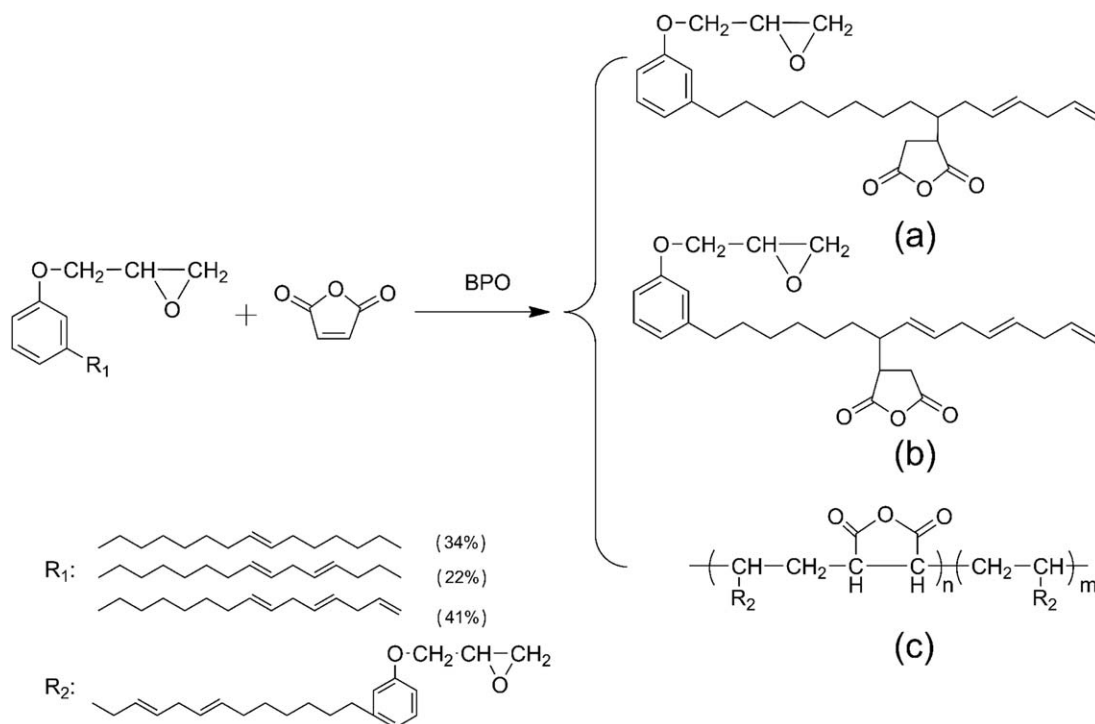


Figure 2. Synthetic routine for M-GPPE.

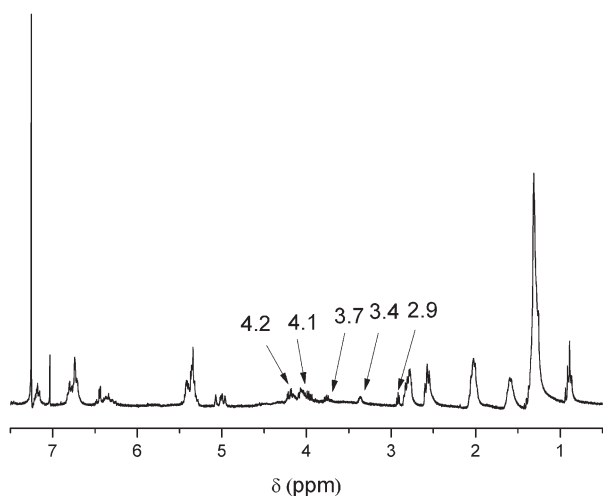


Figure 3. ^1H -NMR spectra of M-GPPE.

membered anhydride.²⁶ All of these results show that the potential structure of M-GPPE in Figure 2(c) existed.

Comparative studies on the thermostability of GPPE and M-GPPE are shown in Figure 4, and the results are summarized in Table I. We observed that the first step in the degradation of GPPE began at 191°C and continued up to 353°C; this corresponded to the decomposition of GPPE long hydrocarbon chain and the glycidyl group of GPPE.²⁴ The value of the weight loss of this stage was reduced significantly by the copolymerization of GPPE with MAH. The second stage of degradation commenced at 353°C and continued up to 600°C because of the decomposition of the GPPE benzene ring.^{22,27} A minor increase in T_{max} and a significant shift toward a lower weight loss of M-GPPE could be explained by the grafting copolymerization of GPPE with MAH. In addition, the first degradation stage of M-GPPE occurred at 100–250°C; this may have been due to the decomposition of unreacted MAH units or MAH copolymers.

Curing Characteristics of the SBR/CB/Silica Compounds

The variation of the curing characteristics of compounds with different plasticizers contents is displayed in Table II. The maximum torque values (M_H) and the minimum torque (M_L) values

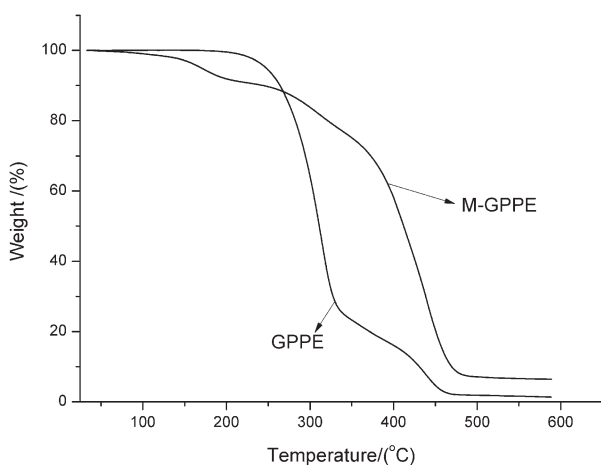


Figure 4. Thermogram of M-GPPE and GPPE.

of the plasticized compounds were lower than the case in the SBR compound without plasticizers. Compared with aromatic oil, the addition of GPPE resulted in a longer t_{90} and lower M_H . Meanwhile, the GPPE plasticized the SBR compound showed the lowest $M_H - M_L$ values, which corresponded to an insufficient crosslinking density of the rubber compounds. However, it has been reported that CNSL plasticized in rubber exhibited a decreasing t_{90} and increasing M_H .^{7,9,10} It was suggested that the epoxy group could easily receive sulfur under the vulcanization accelerators of rubber;¹⁷ this would slow down the curing speed and reduce the crosslinking density of the compounds markedly. Furthermore, the M-GPPE-plasticized SBR complex had a shorter scorch time and t_{90} than GPPE. The phenomenon may have accounted for the occurrence of the esterification reaction between the silica and anhydride group,²⁸ which produced an essential amount of heat²⁹ and supplemented the vulcanization reaction. On the other hand, during the vulcanization process, it was probable that reactions between the epoxy group and anhydride group of M-GPPE or MAH units were carried out;^{30,31} this reduced the effect of epoxy groups on the curing properties of the compounds.

Mechanical Properties of the Composites before and after Aging

In polymer composite studies, the mechanical properties and aging resistance are important parameters in characterization. Table III shows the mechanical properties of the cured rubber specimens before and after aging.

Before aging, the reduction of the hardness and tensile moduli at 100 and 300% for all of the plasticized composites may have been related to the lower degree of crosslinking density in the composites when plasticizers were used. At the same plasticizer loading, the composite plasticized with M-GPPE had higher tensile strength and tear strength values compared with the composites with GPPE and aromatic oil, respectively. The lowest tensile strength and tear strength for the aromatic oil plasticized composite was probably due to the nonpolar character of the aromatic oil. The polarity of the SBR molecular chain was increased by a reaction with GPPE during vulcanization processing; this may have limited reinforced interaction between the SBR chains and silica caused by hydrogen bonding. Thus, the values of the tensile strength and tear strength of the GPPE containing composites were enhanced slightly. However, in the presence of 15 phr of M-GPPE, the tensile strength and tear strength increased by 26 and 23%, respectively. The reason was likely that M-GPPE had a capacity for crosslinking with SBR^{9,10} and for esterification with the silanol group on silica.²⁸ This led

Table I. DTG Analysis of GPPE and M-GPPE

Sample	T_i (°C)	T_f (°C)	T_{max} (°C)	Weight loss (%)
GPPE (first stage)	191	353	302	77
M-GPPE (second stage)	236	344	311	15

T_i : the onset temperature, T_f : the terminal temperature, T_{max} : the maximum decomposition rate temperature.

Table II. Curing Characteristics of the Rubber Compounds

	SBR	Aromatic oil			GPPE			M-GPPE		
		5.0	15	25	5.0	15	25	5.0	15	25
M_L (dN m)	14.86	12.75	10.21	6.23	11.24	8.93	5.76	13.68	11.04	10.11
M_H (dN m)	61.65	50.36	42.71	28.16	42.02	33.27	20.45	52.25	41.23	31.42
t_{10} (min)	0:51	0:51	0:53	1:00	1:02	1:49	2:52	0:58	0:59	1:51
t_{90} (min)	2:27	2:30	2:32	2:32	3:07	4:43	9:53	2:10	3:55	6:56
$M_H - M_L$	46.79	37.61	32.5	21.93	30.78	24.34	14.69	38.57	30.19	21.31

Table III. Mechanical Properties of the Rubbers before and after Aging

	SBR	Aromatic oil			GPPE			M-GPPE			
		5.0	15	25	5.0	15	25	5.0	15	25	
Tensile strength (MPa)	Before aging	16.8	16.0	14.8	14.1	17.6	18.9	15.5	18.7	21.1	17.4
	After aging	15.3	14.4	12.5	11.9	16.5	17.6	14.1	18.3	20.4	17.8
Tearing strength (N/mm)	Before aging	49.8	48.8	45.3	39.7	52.7	49.6	41.9	51.4	61.4	51.1
	After aging	49.3	46.2	43.4	39.5	51.1	46.4	38.6	49.7	58.1	47.6
Elongation at break (%)	Before aging	477	490	590	691	553	693	966	523	620	809
	After aging	367	361	444	477	435	558	740	397	478	577
Modulus at 100% (MPa)	Before aging	2.8	2.5	2.2	1.8	2.2	1.7	1.0	2.6	2.3	1.6
	After aging	4.1	3.6	3.6	3.5	4.0	3.7	3.3	3.9	4.1	3.3
Modulus at 300% (MPa)	Before aging	8.8	8.2	7.1	5.9	7.2	5.8	5.0	8.2	7.7	6.6
	After aging	14.5	14.1	12.7	10.0	11.4	10.6	6.9	14.8	12.1	10.9
Hardness (Shore A)	Before aging	78	75	68	60	72	64	55	76	72	65
	After aging	83	81	79	74	77	73	70	84	82	78

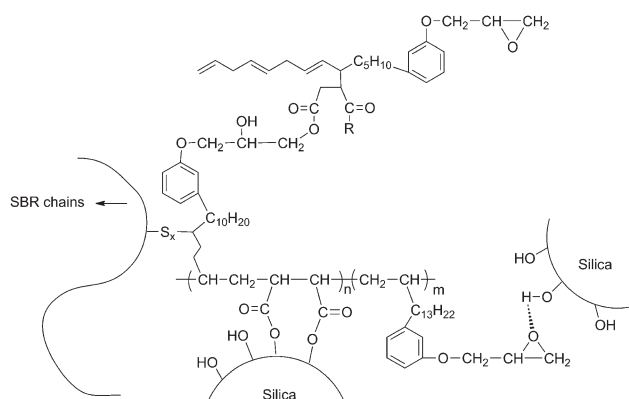
to the enhanced interaction between silica and the rubber molecule chain (Figure 5) and the improved dispersion of silica in the rubber phase. A further increase in the M-GPPE content up to 15 phr decreased both the tensile strength and tearing strength of the composites. Excessive M-GPPE lessened the degree of crosslinking density of the composites substantially and, thus, led to poor mechanical properties, as substantiated previously.

After aging, although the tensile strength and the elongation at break of the composites plasticized with GPPE and M-GPPE dropped markedly, the reduction was less than in the case of aromatic oil, especially at higher plasticizer loadings. Whereas the tensile strength retention and tear strength retention were used to evaluate the anti-aging performance of these composites, the results of the composites with GPPE and M-GPPE showed a high anti-oxidative ability that was equal to or better than that in many early works.^{2,7,32,33} This may have been related to the decrease in the number of unstructured bonds of SBR through the reaction with GPPE and M-GPPE.

Morphology

To determine the dispersion of silica, TEM analysis of the samples was performed. Figure 6 shows the TEM photographs of the SBR/CB/silica composites with or without plasticizers. Figure 6(a,b) demonstrates that there were a lot of agglomerates

with large sizes of greater than 100 nm; this suggested the poor dispersion of silica in rubber. On the other hand, it was clear that the agglomerate size significantly decreased and the particles of silica were uniformly dispersed in the rubber matrix with the introduction of GPPE [Figure 6(c)] and M-GPPE [Figure 6(d)], respectively. This confirmed that the increases in the tensile strength and tear strength of the composite plasticized with M-GPPE was caused by the decreasing size of the agglomerate.

**Figure 5.** Schematic interfacial structure between the silica and SBR chains.

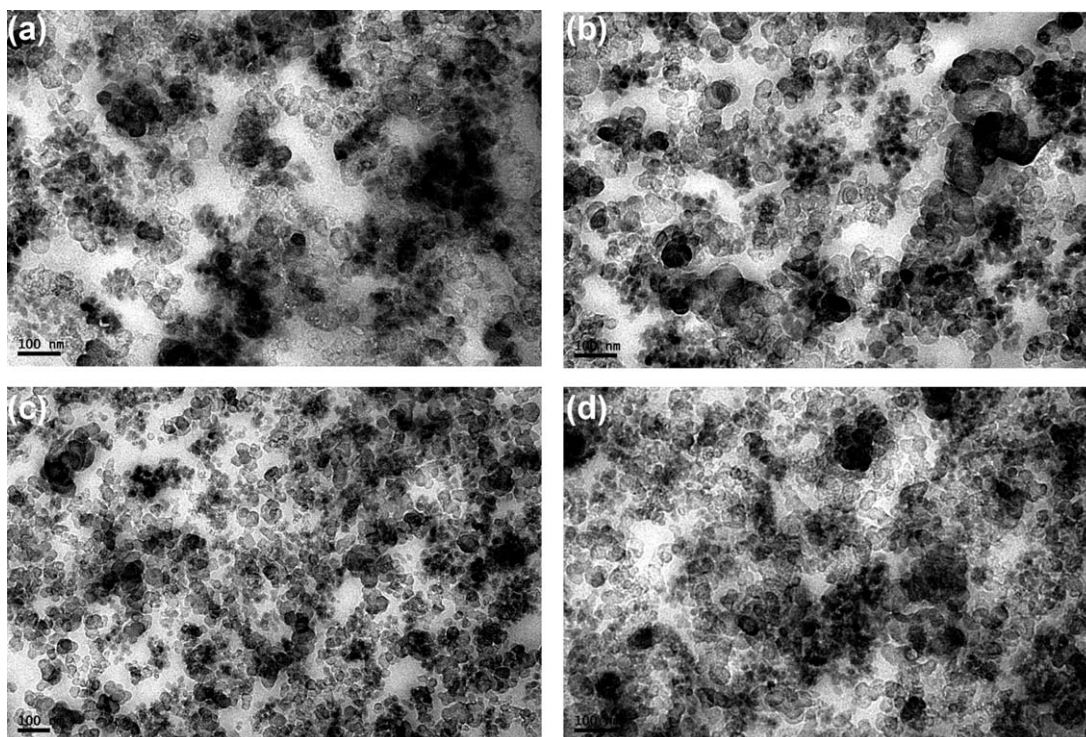


Figure 6. TEM images of the composites with different plasticizers (15 phr) or without a plasticizer: (a) without a plasticizer, (b) aromatic oil, (c) GPPE, and (d) M-GPPE.

Dynamic Performance of the Composites

The addition of plasticizers had a substantial influence on the static and dynamic behavior of the polymer. Figure 7 shows the dynamic viscoelastic properties as a function of the temperature of the SBR composites without or with 15 phr plasticizers. As shown in Figure 7(a), the loss modulus (G'') of the composites decreased with the addition of plasticizers in the temperature range of -5 to 80°C . It was suggested that the filler network could be weakened, and the energy loss from the friction of the SBR molecular chains with filler particles was reduced in the presence of plasticizers, which played the role as the lubricant in SBR. It could also be seen that the G'' of the composites containing GPPE was lower than those of aromatic oil and M-GPPE because of the lowest crosslinking density of the former. Compared to aromatic oil, M-GPPE resulted in a higher G'' value in the composites. The potential reason for this result was that M-GPPE enhanced the frictional losses between the silica and rubber matrix, and this led to a higher G'' , as in the study of Suphadon et al.³⁴

The glass-transition temperature of each composite corresponded to the temperature, and this showed its maximum loss factor value. The loss factor curves of the composites are shown in Figure 7(b). The composite plasticized with GPPE showed the lowest glass-transition temperature followed by with M-GPPE, with aromatic oil, and without plasticizer from low to high. This result corresponded to the curing characteristics of the compounds with tendencies of crosslinking density of the compounds of With GPPE < With M-GPPE < With aromatic oil < Without plasticizer. Lower glass-transition temperature of the composites plasticized with M-GPPE was indicated that the cold resistance was better than the composite plasticized with aromatic oil.

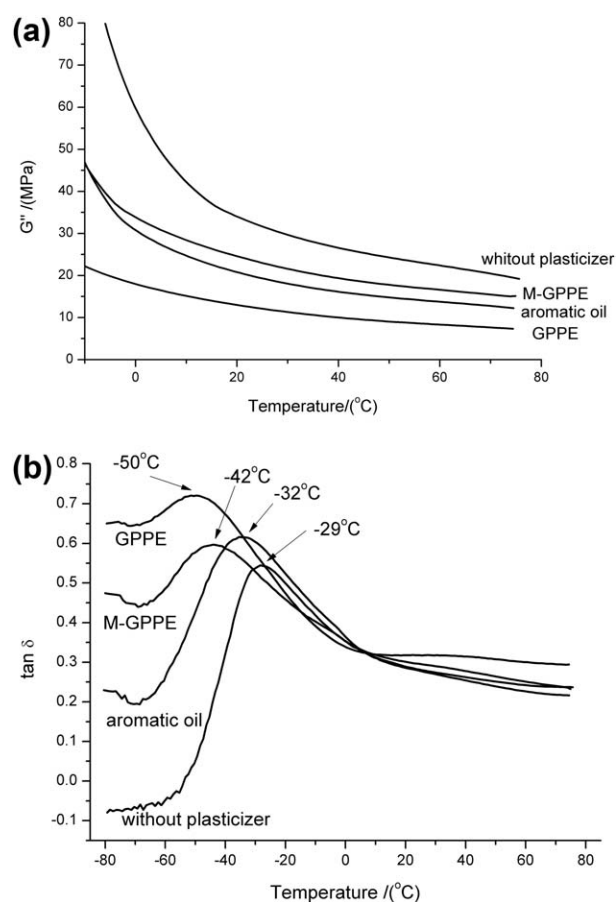


Figure 7. (a) G'' and (b) loss factor for composites with different plasticizers.

Noticeably, the values of the loss factor at 60°C for SBR without plasticizer, with aromatic oil, with GPPE, and with M-GPPE were 0.24, 0.22, 0.30, and 0.25, respectively. The loss factor value of the M-GPPE composite was lower than the GPPE composite but slightly higher than those with aromatic oil and without plasticizer, whereas the presence of M-GPPE provided a better dispersion of silica with a higher mechanical strength than the others. Three factors may have been responsible for these results. First, the CB network in the composite was undermined by the addition of aromatic oil. Second, the silica–silica interaction was weakened by the addition of GPPE and M-GPPE, especially M-GPPE. Finally, interfacial interactions via covalent bonding or noncovalent bonding, such as hydrogen bonding, may have led to a higher hysteresis.³⁵ Furthermore, because the M-GPPE was a branchy copolymer, aggravated interfacial chain motion may have led to higher loss around 60°C.³⁶

CONCLUSIONS

We drew the following conclusions from this study: the monomer of GPPE were polymerized by free-radical polymerization with MAH into a polymer of M-GPPE, and the thermostability of GPPE was improved by grafting copolymerization with MAH. The curing time for the compound did not change significantly with the incorporation of M-GPPE, whereas it increased significantly with GPPE. SBR/CB/silica composites plasticized with M-GPPE exhibited better dynamic properties and mechanical properties, including tensile strength and tearing strength, than the composites with GPPE. Compared to aromatic oil, M-GPPE had equivalent values of curing characteristics and dynamic properties but better mechanical properties and hot-air aging properties. TEM analysis showed that M-GPPE improved the dispersion of silica in the SBR rubber phases and enhanced the interaction between the filler and rubber phases. M-GPPE can be considered a renewable reactive plasticizer for SBR/polar filler composites with great application potential.

REFERENCES

1. Sreenivasan, P.; Ratna, D.; Albert, P.; Somashekaran, J. *J. Appl. Polym. Sci.* **2013**, *128*, 2414.
2. Noriman, N. Z.; Ismail, H. *J. Appl. Polym. Sci.* **2012**, *124*, 19.
3. Pan, Q. W.; Wang, B. B.; Chen, Z. H.; Zhao, J. Q. *Mater. Des.* **2013**, *50*, 558.
4. Bhunia, H. P.; Jana, R. N.; Basak, A.; Lenka, S. *J. Polym. Sci. Part A: Polym. Chem.* **1988**, *36*, 391.
5. Nimuru, N.; Miyakoshi, T. *Int. J. Polym. Anal. Charact.* **2003**, *8*, 47.
6. Sultania, M.; Rai, J. S. P.; Srivastava, D. *Int. J. Chem. Kinet.* **2009**, *41*, 559.
7. Mary, A.; Thachil, E. T. *J. Appl. Polym. Sci.* **2006**, *102*, 4835.
8. Fernando, G.; Souza, J.; José, C. P.; Oliveirab, G. E.; Soaresb, B. G. *Polym. Test.* **2007**, *26*, 720.
9. Arayaprane, W.; Rempel, G. L. *J. Appl. Polym. Sci.* **2007**, *106*, 2696.
10. Menon, A. R. R.; Sonia, T. A.; Sudha, J. D. *J. Appl. Polym. Sci.* **2006**, *102*, 5123.
11. Chuayjuljit, S.; Rattanametangkool, P.; Potiyaraj, P. *J. Appl. Polym. Sci.* **2007**, *104*, 1997.
12. Greco, A.; Brunetti, D.; Renna, G.; Mele, G.; Maffezzoli, A. *Polym. Degrad. Stab.* **2010**, *95*, 2169.
13. Chakrawarti, P.; Mehta, V. *Ind. J. Technol.* **1997**, *25*, 109.
14. Sultania, M.; Rai, J. S. P.; Srivastava, D. *Hazard J. Mater.* **2011**, *185*, 1198.
15. Henne, M.; Breyer, C.; Niedermeir, M.; Ermanni, P. A. *Polym. Compos.* **2004**, *25*, 255.
16. Kamal, K. K.; Sharma, S. D.; Suraj, K. B.; Prashant, K. *Curr. Sci.* **2006**, *90*, 1492.
17. Zhang, G. P.; Cheng, J.; Shi, L.; Lin, X. *Thermochim. Acta* **2012**, *538*, 36.
18. Dharmarajan, N.; Datta, S. *Polymer* **1992**, *33*, 3848.
19. Stretz, H. A.; Paul, D. R. *Polymer* **2006**, *47*, 8527.
20. Vikram, T.; Nando, G. B. *J. Appl. Polym. Sci.* **2007**, *105*, 1280.
21. Barton, J. M.; Greenfield, D. C. L. *Br Polym J* **1986**, *18*, 51.
22. Madhusudhan, V.; Murthy, B. G. K. *Prog. Org. Coat.* **1992**, *20*, 63.
23. Nakason, C.; Saiwaree, S.; Tatun, S.; Kaesaman, A. *Polym. Test.* **2006**, *25*, 656.
24. Bhunia, H. P.; Nandoa, G. B.; Basakb, A.; Lenkac, S.; Nayakc, P. L. *Eur. Polym. J.* **1999**, *351*, 713.
25. Kattimuttathu, I. S.; Vadi, S. *Ind. Eng. Chem. Res.* **2005**, *44*, 4504.
26. Pinyo, W.; Charoen, N.; Qinmin, P.; Garry, L. R. *Eur. Polym. J.* **2013**, *49*, 4035.
27. Symes, W. F.; Dawson, C. R. *J. Am. Chem. Soc.* **1953**, *75*, 4952.
28. Tai, Y. L.; Qian, J. S.; Zhang, Y. C.; Huang, J. D. *Chem. Eng. J.* **2008**, *141*, 354.
29. Rocks, J.; Rintoula, L.; Vohwinkelc, F.; George, G. *Polymer* **2004**, *45*, 6799.
30. Sun, G.; Sun, H.; Liu, Y.; Binyuan, Z.; Na, Z.; Keao, H. *Polymer* **2007**, *48*, 330.
31. Varshney, A.; Mohan, M. R.; Prajapati, K. *Int. J. Chem.* **2012**, *4*, 113.
32. Abdelwahab, N. A.; El-Nashar, D. E.; Abd El-Ghaffar, M. A. *Mater. Des.* **2011**, *32*, 238.
33. Abd El-Ghaffar, M. A.; El-Nashar, D. E.; Youssef, E. A. M. *Polym. Degrad. Stab.* **2003**, *82*, 47.
34. Suphadon, N.; Thomas, G. J.; Busfield, J. C. *Polym. Test.* **2010**, *29*, 440.
35. Lei, Y. D.; Tang, Z. H.; Guo, B. C.; Zhu, L. X.; Jia, D. M. *Express Polym. Lett.* **2010**, *4*, 692.
36. Lei, Y. D.; Tang, Z. H.; Guo, B. C.; Jia, D. M. *Polym. J.* **2010**, *42*, 555.